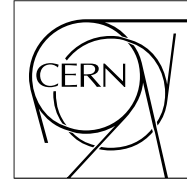


The Compact Muon Solenoid Experiment
Analysis Note

The content of this note is intended for CMS internal use and distribution only



September 25, 2007

Dijet Ratio from QCD and Contact Interactions

Manoj K. Jha

University of Delhi , India and INFN, Bologna, Italy

Robert M. Harris

Fermilab, Batavia, IL, USA

Marek Zieliński

University of Rochester, Rochester, NY, USA

Abstract

Using CMSSW, we have studied CMS sensitivity to contact interactions based on the dijet ratio: the ratio of dijet-mass cross sections in two different rapidity regions within the CMS barrel. We confirmed and extended the results published in Physics TDR II [1]. Sensitivity to contact interaction signal has been enhanced after optimization of η cuts. With only 10 pb^{-1} of data, CMS will be sensitive to a contact interaction beyond the present Tevatron limit. For an integrated luminosity of 10 pb^{-1} , 100 pb^{-1} , and 1 fb^{-1} , CMS can expect to exclude at 95% CL a contact interaction scale Λ of 5.3, 8.3, and 12.5 TeV or discover at 5σ significance a scale Λ of 4.1, 6.8 and 9.9 TeV, respectively.

1 Introduction

The first observation of the size of atomic nucleus was obtained by Geiger and Marsden in the Rutherford [2] scattering of α particles from nuclei. In an analogous way, we could discover a non-zero quark radius by observing the scattering of the highest energy partons in pp collision at the LHC collider. In quantum chromodynamics (QCD), parton-parton scattering processes are mainly t-channel exchanges and produce angular distributions of dijets (ie. the two leading jets in the event) peaked at small center-of-mass scattering angles; many processes containing new physics are more isotropic. Thus the dijet angular distribution provides an excellent test of QCD dynamics and a means of searching for new physics at a mass scale (Λ) which characterizes the strength of quark-substructure binding interactions and the physical size of the composite states. New physics at a scale Λ , above the mass of the directly reachable final states, is effectively modeled as a contact interaction.

This analysis focuses on CMS sensitivity to quark compositeness using the formalism of Eichten et al. [3, 4, 5]. In this formalism, the Lagrangian incorporates the compositeness of left-handed quarks in the left-left isoscalar term

$$L_{qq} = A(g^2/2\Lambda_{LL}^2)\bar{q}_L\gamma^\mu q_L\bar{q}_L\gamma_\mu q_L,$$

where $A = \pm 1$ is the sign of the interference term, Λ_{LL} is the compositeness scale, and the dependence on α_s is contained in the compositeness coupling constant g^2 . The model is completely determined by specifying the two parameters A and Λ_{LL} . An earlier study towards CMS sensitivity to such quark contact interactions using ORCA can be found in [6].

2 Analysis Procedures

2.1 Monte Carlo Samples

This analysis employs Monte Carlo QCD event samples produced for the Software and Detector Performance Validation (SDPV) exercise using CMSSW_1.2.0. The particle-level events were generated with PYTHIA 6.227 [7] using the Tune DWT for Underlying Event parameters [8]. The CMS detector simulation as implemented in CMSSW_1.2.0 based on the GEANT4 package was used to simulate passage of particles through the detector and the energy deposits in the sensitive volumes. All the results which are presented here have been derived from samples without pileup. QCD dijet samples were generated in 21 bins of the momentum transfer in the parton hard-scatter, \hat{P}_T , which span the full kinematic range. Each sub-sample has a weight corresponding to the generated cross section for that sub-sample. To obtain the dijet ratio distributions, all events from each sub-sample are used along with their corresponding weights and errors are calculated taking into account the weights.

We generated the QCD plus a contact interaction samples using PYTHIA in CMSSW with the same settings as for the QCD samples described above, except for including the contact interaction term. We chose the variant of the model where all three families of quarks are assumed to be composite and used $A = +1$ parameter, corresponding to destructive interference. Since the analysis of the QCD samples indicated good agreement between results from generated and corrected calorimeter levels, we did not employ the full detector simulation for the contact interaction samples, and used the generated-level distributions instead.

2.2 Jet Reconstruction

Jet reconstruction and performance in CMSSW_1_2_0 is presented in [9]. Here, we use the Midpoint cone algorithm with cone radius in $\eta - \phi$ space of $R = 0.5$ for reconstructing jets at generated (GenJets) and calorimetry (CaloJets) levels. Scheme B cell thresholds [10] are applied when reconstructing CaloJets. Since jet response is not constant with respect to η , Monte Carlo jet energy corrections [9] have been applied to CaloJets to obtain the corrected jets (CorJets).

2.3 Analysis Software

The CMSSW module used to make the dijet mass and dijet ratio distributions can be found in the package RecoJets/JetAnalyzers. The source code is `src/DijetRatio.cc`, and the header which defines the mass binning is `interface/DijetRatio.h`. In the sub-directory `test/DijetRatio` are files for running the jobs. The `cfg` file for running a job is created with `submitDiJetAnalysis.csh` for a specified \hat{p}_T bin and inner and outer η cut, and the job is run in a batch queue via `condor-submit-diJetAnalysis.csh`. This job runs on a CMSSW_1_2_0 sample that contains GenJets, CaloJets and Corrected CaloJets. The script job-submission is an example of submitting jobs for all \hat{p}_T bins and an inner cut of 0.5 and an outer cut of 1.0. This creates a root file for each \hat{p}_T , which are renamed to have sequential numbers using `moving.csh`, and then read and analyzed using the root script `MassAnaBackgrd.C`, which applies the cross section weights stored in the file `datasetBackgrd.txt`. The source code `DijetRatio.cc` simply makes histograms of rate vs. dijet mass for the input η cuts, which are written to root files, and the root script `MassAnaBackgrd.C` then does the bulk of the analysis, including forming the ratio. This procedure was used by Manoj Jha with CMSSW_1_2_0, and all code builds with both CMSSW_1_2_X and CMSSW_1_3_X.

3 Contact Interaction Searches with Dijets

This analysis employs dijet systems consisting of the two jets with the highest transverse momenta in the event (the two leading jets). The dijet events are defined as $pp \rightarrow 2 \text{ leading jets} + X$, where X can be anything, including additional jets.

3.1 Dijet Mass

In the presence of a contact interaction, we expect an increase in the event rate relative to QCD at high dijet mass. The dijet invariant mass is defined as $M = \sqrt{(E_1 + E_2)^2 - (\vec{P}_1 + \vec{P}_2)^2}$. The dijet mass distributions resulting from quark contact interactions with different values of compositeness scale Λ are compared to QCD distribution generated with Pythia [7] in Fig. 1. The contact interaction rate increases at higher mass and for smaller compositeness scales the effect is larger. However, observation of contact interactions in the mass distribution is difficult because there are large systematic uncertainties in the measurement and in the QCD calculation of the cross-section as a function of dijet mass. The steeply falling QCD spectrum is sensitive to jet energy uncertainties, resulting in large uncertainties in the cross-section.

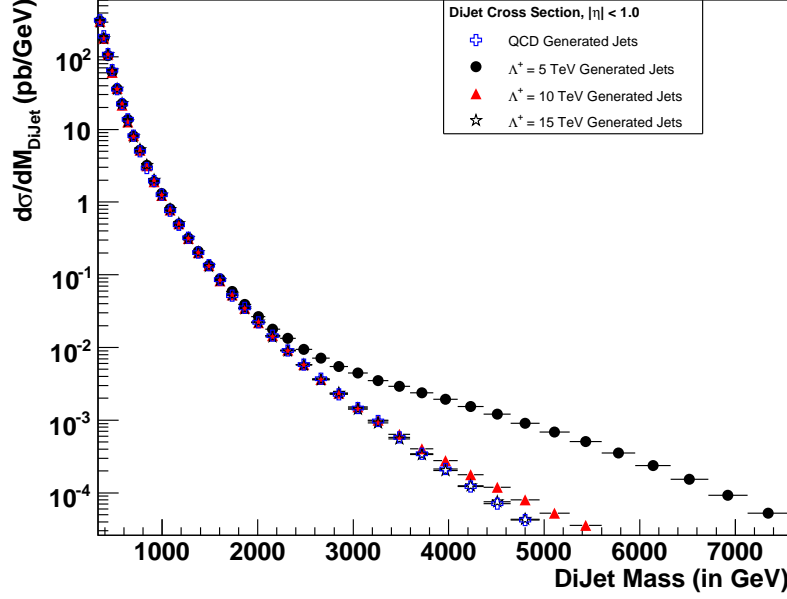


Figure 1: Simulation of the dijet mass distribution from QCD and from QCD plus contact interaction with scales of 5, 10, and 15 TeV.

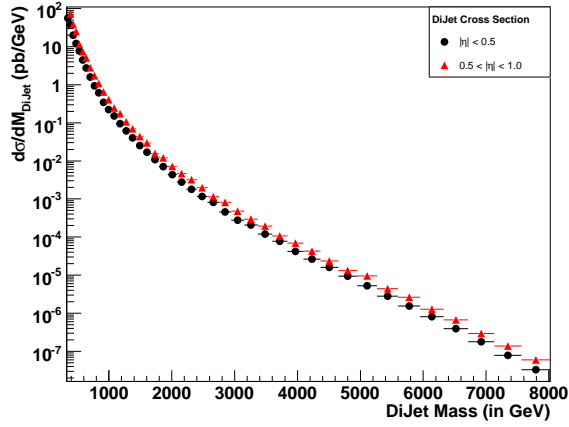
3.2 Dijet Ratio

To characterize the shape of the angular distribution in a mass bin, we use the variable $R = N(|\eta| < \eta_1)/N(\eta_1 < |\eta| < \eta_2)$, the ratio of the number of dijet events with $|\eta| < \eta_1$ to the number of dijet events with $\eta_1 < |\eta| < \eta_2$. In the following discussion, we initially adopt the values of $\eta_1 = 0.5, \eta_2 = 1.0$ which were used in the original $D\bar{O}$ analysis [11] and then optimize these values within the CMS barrel region. Figures 2(a) and 2(b) show the cross-sections for QCD and QCD plus a contact interaction, respectively, in the inner ($|\eta| < \eta_1$) and outer ($\eta_1 < |\eta| < \eta_2$) regions. The cross-section for QCD is peaked in the outer region due to t-channel exchange of gluons among point-like quarks. In contrast, the cross-section is increased in the inner region for QCD plus a contact interaction since it originates from more isotropic interactions.

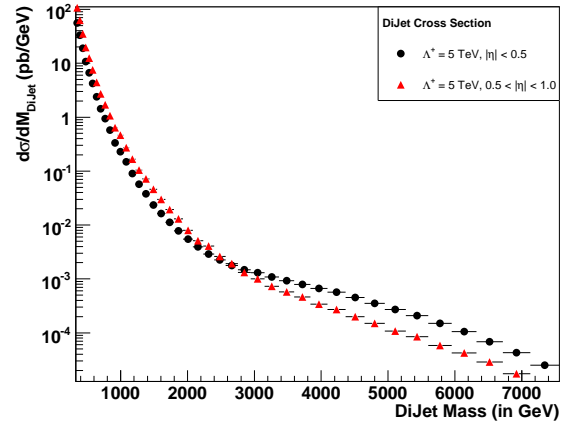
Figures 3(a) and 3(b) depict the dijet ratio from QCD and QCD plus contact interaction at initial parton and at particle-jet levels. There is a good agreement between dijet ratio distributions at parton and particle levels in the low dijet mass region, while a deviation of 5% is seen at higher dijet mass. QCD alone gives a fairly flat dijet ratio around 0.6. For QCD plus contact interaction, the ratio increases with dijet mass for a given compositeness scale, and decreases at large mass with increase in the compositeness scale.

4 Results

To evaluate the statistical sensitivity to contact interactions in the early running period of CMS, we focus on the results for the integrated luminosity values of $10 \text{ pb}^{-1}, 100 \text{ pb}^{-1},$ and 1 fb^{-1} . However, we include some selected results for 10 fb^{-1} as well.

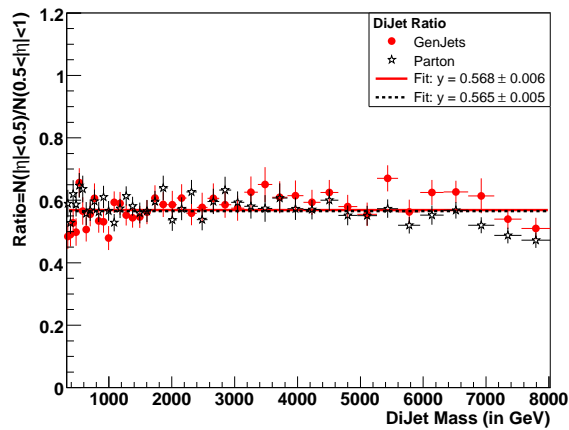


(a) QCD

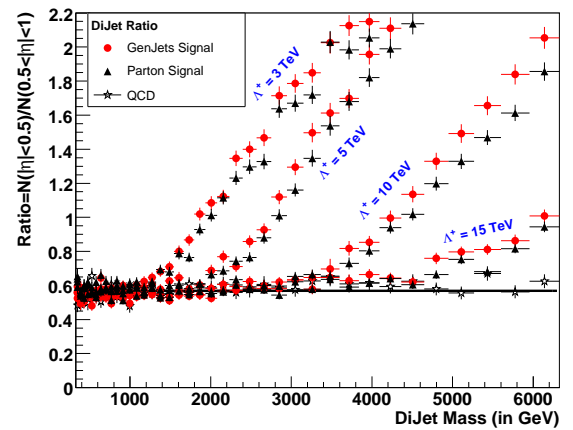


(b) QCD plus contact interaction

Figure 2: Simulation of dijet mass distribution in the inner and outer regions of the CMS barrel for QCD (2(a)) and QCD plus a quark contact interaction (2(b)).



(a) QCD



(b) QCD plus contact interaction

Figure 3: Simulation of dijet ratio at parton and particle-jet levels for QCD (3(a)) and QCD plus a contact interaction (3(b)).

4.1 Statistical Uncertainties for Dijet Ratios

Figure 4 shows the dijet ratio from full CMS detector simulation for jets at generated, calorimetry and corrected calorimetry levels. The dijet ratios from corrected CaloJets and from generated jets are similar at 0.6. The ratio from CaloJets is shifted due to variation of the jet response versus η .

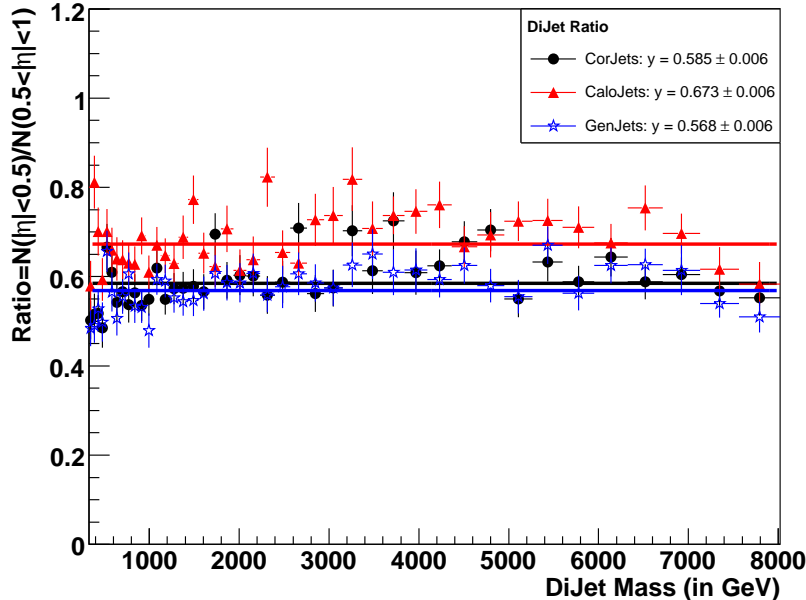
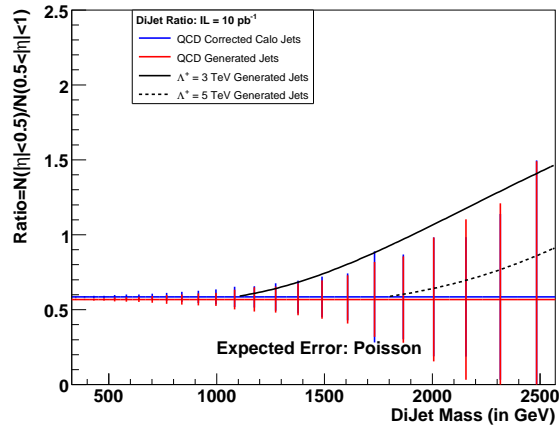


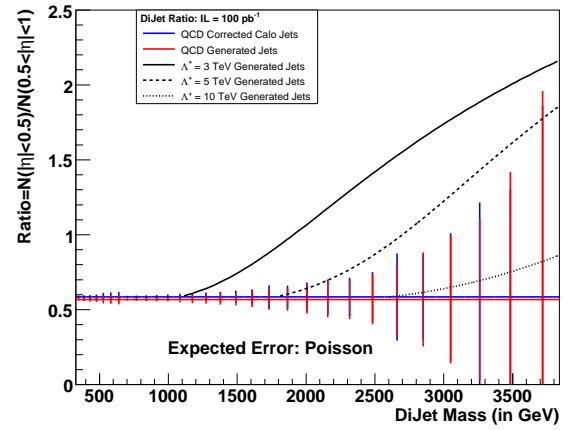
Figure 4: Simulation of dijet ratio from QCD for GenJets, CaloJets, and CorJets.

Figure 5 presents the predicted dijet ratios for QCD and QCD plus a contact interaction; the statistical uncertainties shown are smooth estimates expected for the above four luminosity values and the jet trigger table proposed in reference [12]. The calculation of the statistical uncertainties is discussed in [6]. We use Poisson statistics at high dijet mass where few events are expected. For all four integrated luminosities, the highest mass bin shown in Fig. 5 has a mean value of expected QCD background events in the numerator of approximately 1.5 events, and 2.5 events in the denominator.

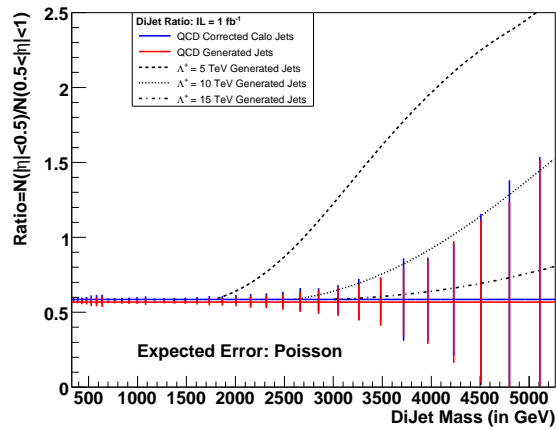
Comparing the contact interaction signals in Fig. 5 to the QCD background and its statistical uncertainty indicates CMS level of sensitivity expected for contact interactions. For 10 pb^{-1} , it will be difficult to discover or exclude $\Lambda = 5 \text{ TeV}$, which is too close to QCD, but we expect sensitivity to roughly $\Lambda = 3 \text{ TeV}$ at high mass. The Tevatron limit on compositeness scale is 2.7 TeV at 95% confidence level (CL) for integrated luminosity of 100 pb^{-1} . For 100 pb^{-1} , we expect to discover or exclude $\Lambda = 5 \text{ TeV}$. For 1 fb^{-1} , statistical errors are reduced at high mass, and should be sensitive to roughly $\Lambda = 10 \text{ TeV}$. For 10 fb^{-1} the statistical errors are reduced again, and we expect sensitivity to $\Lambda = 15 \text{ TeV}$.



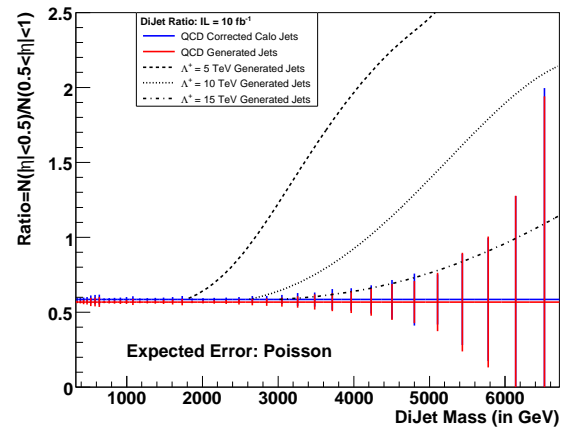
(a) 10 pb^{-1}



(b) 100 pb^{-1}



(c) 1 fb^{-1}



(d) 10 fb^{-1}

Figure 5: Dijet Ratio of QCD is compared with QCD plus a contact interaction for four values of integrated luminosity.

4.2 Estimates of Sensitivity to Contact Interaction

For quantitative estimates of sensitivity to contact interactions, we form a χ^2 between QCD plus a contact interaction and QCD alone (based on statistical uncertainties only). This χ^2 is subsequently used to estimate the Λ values we expect to exclude at 95% CL and the Λ values we expect to discover at 5σ .

Table 1 shows the χ^2 (using statistical uncertainties only) between QCD plus a contact interaction and QCD alone:

$$\chi^2 = \sum_i \frac{\Delta_i^2}{\sigma_i^2} \quad (1)$$

where for each bin i , Δ_i is the difference between QCD plus a contact interaction and QCD only, and σ_i is the statistical uncertainty on QCD background, as shown in Fig. 5. Since we use smooth estimates for both the background and the signal, the χ^2 tends to zero when the contact interaction scale is very large ($\Lambda \rightarrow \infty$) and the signal distribution becomes identical to QCD. This is different than a χ^2 in the presence of actual statistical fluctuations, which is seldom expected to be zero.

Luminosity	10 pb ⁻¹				100 pb ⁻¹				1 fb ⁻¹			
Λ (TeV)	3	5	10	15	3	5	10	15	3	5	10	15
χ^2 (stat)	16.07	0.42	0.002	5.4×10^{-5}	281.2	21.75	0.205	0.036	3236	406.5	10.24	1.135

Table 1: χ^2 between QCD (background) and QCD plus a contact interaction (signal).

In Figure 6, we plot the significance versus $1/\Lambda$. As discussed, $1/\Lambda = 0$ corresponds to QCD alone (ie. no contact interaction contribution), and we observe a $\chi^2 = 0$ and a significance of 0σ as expected. A 95% CL exclusion corresponds to a significance of 1.96σ for a two sided Gaussian probability for the signal. The 95% CL and the 5σ discovery level are shown by horizontal dotted lines in Fig. 6. For integrated luminosities of 10 pb⁻¹, 100 pb⁻¹, and 1 fb⁻¹, we determine the significance for four different values of $\Lambda = 3, 5, 10$, and 15 TeV. A fit to the four $1/\Lambda$ points shown in Fig. 6 is used to find the 95% CL and 5σ values of Λ . In Table 2 we list the resulting Λ values for a 95% CL exclusion or 5σ discovery (using statistical uncertainties only).

	95% CL Excluded Scale			5σ Discovered Scale		
	10 pb ⁻¹	100 pb ⁻¹	1 fb ⁻¹	10 pb ⁻¹	100 pb ⁻¹	1 fb ⁻¹
Λ (TeV)	< 3.8	< 6.8	< 12.2	< 2.8	< 4.9	< 9.1

Table 2: Sensitivity to contact interactions with 10 pb⁻¹, 100 pb⁻¹, and 1 fb⁻¹. Estimates include statistical uncertainties only.

4.3 Optimization of η Cuts within the Barrel

In previous Sections, we have used the η cuts from Tevatron for calculating the dijet ratio from QCD and QCD plus a contact interaction. Here, we optimize the η cuts to maximize the sensitivity of the signal with respect to the background within the barrel region of the CMS calorimeter. To have optimal sensitivity early in CMS running, we

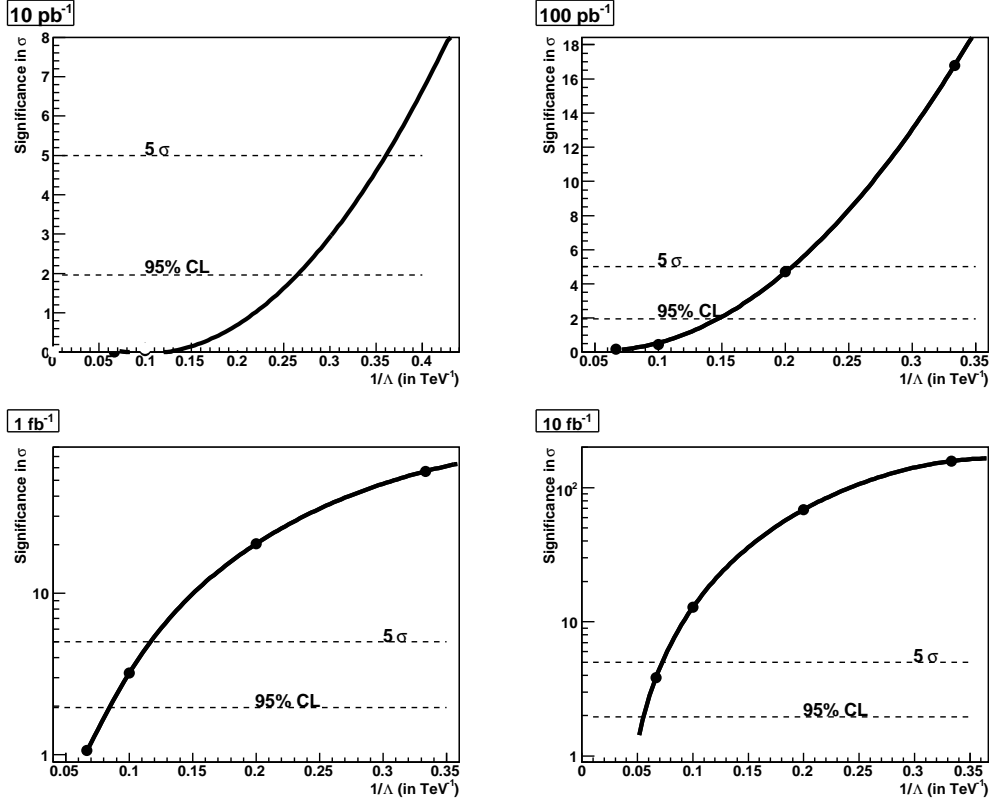


Figure 6: Significance (using statistical uncertainties only) of the difference between QCD and QCD plus a contact interaction for integrated luminosities of 10 pb^{-1} , 100 pb^{-1} , 1 fb^{-1} , and 10 fb^{-1} . The significance is plotted vs $1/\Lambda$ and is fitted with a smooth function. Horizontal lines show the 5σ and 95% CL levels. Log scales are used where necessary to view the 5σ and 95% CL levels.

optimize for an integrated luminosity of 100 pb^{-1} and a contact interaction of $\Lambda = 5 \text{ TeV}$. For this optimization, only points for dijet masses $> 1.8 \text{ TeV}$ are included in the χ^2 .

Table 3 shows the χ^2 values as function of inner and outer η cuts. We have considered the outer η cut (first row) from 0.9 to 1.3 while the inner η cut (first column) varies from 0.3 to 0.9 in steps of 0.1. The outer η cut of 1.3 corresponds to maximum value to stay within the barrel. This value also corresponds to the optimal choice of η cut for dijet resonances searches [13]. The optimized η cuts correspond to maximum sensitivity, ie. maximum χ^2 . The maximum value of χ^2 is 199.9 and it corresponds to η outer (η_o) and η inner (η_i) of 1.3 and 0.7 respectively.

Figure 7 shows the dijet ratio from full CMS detector simulation for jets at generated, calorimetry and corrected calorimetry levels for the optimized η cuts. The dijet ratio from corrected CaloJets and generated jets are similar at 0.5. Figure 8 shows the dijet ratio from QCD and QCD plus a contact interaction for the η cuts from Tevatron and for the optimized η cuts. The signal sensitivity for the optimized η cuts has been enhanced with respect to the η cut from Tevatron. Figure 9 presents the dijet ratio for QCD and QCD plus a contact interaction for the optimized η cuts and for the four values of integrated luminosity. Again, the sensitivity to signal for the optimized η cuts has been enhanced comparing to Fig. 5. The significance versus $1/\Lambda$ is shown in Fig 10. Table 4 lists the χ^2 values (using statistical uncertainties only) between QCD and QCD plus a contact interaction for the optimized η cuts.

	0.9	1.0	1.1	1.2	1.3
0.3	4.6	9.8	19.8	32.0	44.9
0.4	7.0	16.6	34.5	56.3	80.6
0.5	9.1	20.4	55.1	91.6	128.9
0.6	9.1	21.9	63.6	129.6	182.3
0.7	4.2	13.7	54.8	116.1	199.9
0.8		12.7	50.1	101.8	170.8
0.9			35.7	86.4	145.3

Table 3: χ^2 between QCD and QCD plus a contact interaction as function of inner (first column) and outer (first row) η cuts for 100 pb^{-1} and $\Lambda = 5 \text{ TeV}$.

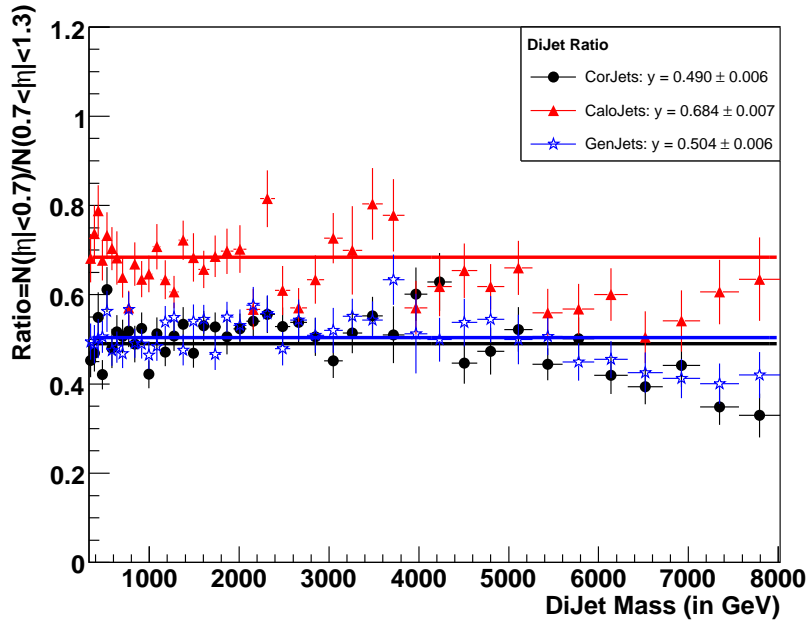
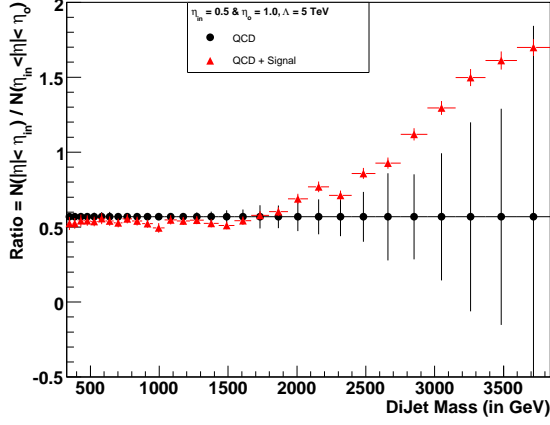
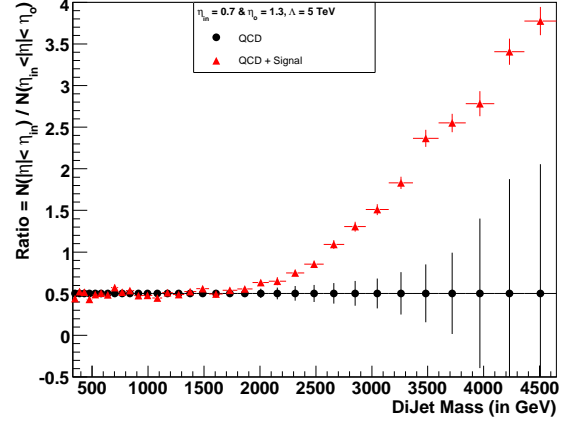


Figure 7: Simulation of dijet ratio from QCD for GenJets, CaloJets, and CorJets for the optimized η cuts.

(a) η cuts from Tevatron(b) Optimized η cutsFigure 8: Dijet ratio for the η cuts from Tevatron and for the optimized η cuts.

Luminosity	10 pb ⁻¹				100 pb ⁻¹				1 fb ⁻¹			
Λ (TeV)	3	5	10	15	3	5	10	15	3	5	10	15
χ^2 (stat)	151	5.6	0.01	0.0001	2450	169.1	0.5594	0.0054	2.83e+04	3005	22.32	0.4271

Table 4: χ^2 between QCD (background) and QCD plus a contact interaction (signal) for the optimized η cuts.

	95% CL Excluded Scale			5 σ Discovered Scale		
	10 pb ⁻¹	100 pb ⁻¹	1 fb ⁻¹	10 pb ⁻¹	100 pb ⁻¹	1 fb ⁻¹
Λ (TeV)	< 5.3	< 8.3	< 12.5	< 4.1	< 6.8	< 9.9

Table 5: Sensitivity to contact interactions with 10 pb⁻¹, 100 pb⁻¹, and 1 fb⁻¹ for the optimized η cuts. Estimates include statistical uncertainties only.

Finally, Table 5 lists the values of Λ that correspond to 95% CL exclusion and 5 σ discovery limits.

5 Conclusion

Using CMSSW, we have studied CMS sensitivity to contact interactions based on the dijet ratio from QCD and contact interaction. We confirmed and extended the results published in Physics TDR II [1]. With only 10 pb⁻¹ of data, CMS will be sensitive to a contact interaction beyond the present Tevatron limit. We optimized the η cuts used for calculating the dijet ratio for best sensitivity to contact interactions. Consequently, the sensitivity to contact interaction signal has been enhanced after optimization of η cuts. For an integrated luminosity of 10 pb⁻¹, 100 pb⁻¹, and 1 fb⁻¹, CMS can expect to exclude at 95% CL a contact interaction scale Λ of 5.3, 8.3, and 12.5 TeV or discover at 5 σ significance a scale Λ of 4.1, 6.8 and 9.9 TeV, respectively.

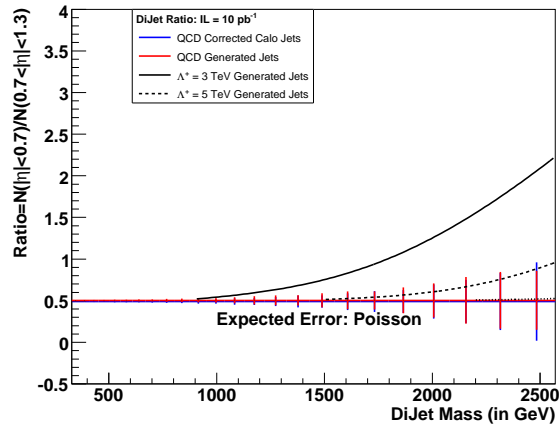
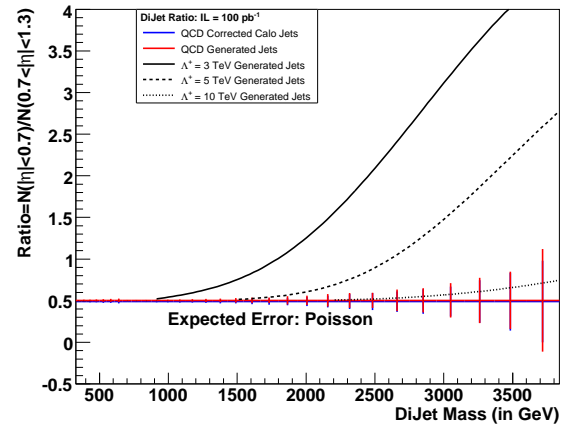
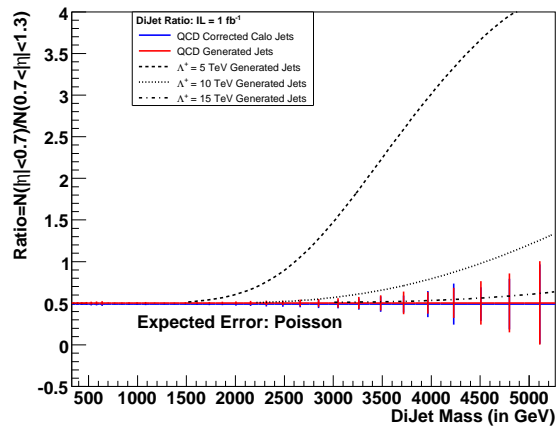
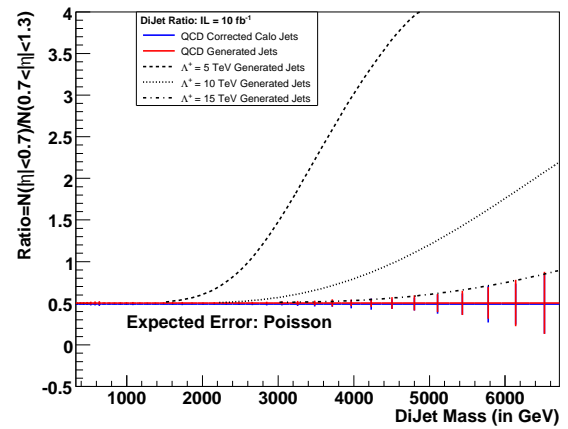
(a) 10 pb^{-1} (b) 100 pb^{-1} (c) 1 fb^{-1} (d) 10 fb^{-1}

Figure 9: Dijet Ratio of QCD is compared with QCD plus a contact interaction for the optimized η cuts and four values of integrated luminosity.

This analysis demonstrates that dijet measurements at CMS can provide an early signal of physics beyond the Standard Model.

References

- [1] **J. Phys. G: Nucl. Part. Phys.** **34** 995-1579 CMS Collaboration 2007, *CMS Technical Design Report, Volume II: Physics Performance*
- [2] **Cambridge University Press, Cambridge, England, 1930**, E. Rutherford, J. Chadwick, and C. D. Ellis, “*Radiations from Radioactive Substances*”.

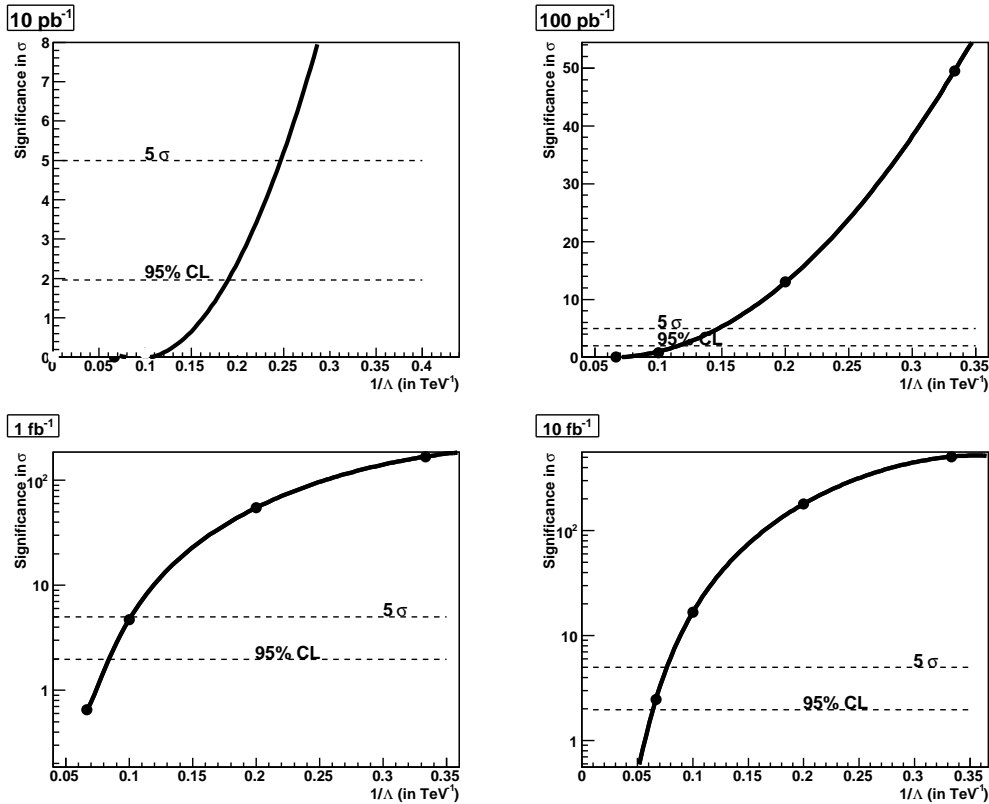


Figure 10: Significance (using statistical uncertainties only) of the difference between QCD and QCD plus a contact interaction for integrated luminosities of 10 pb^{-1} , 100 pb^{-1} , 1 fb^{-1} , and 10 fb^{-1} for the optimized η cuts. The significance is plotted vs $1/\Lambda$ and fitted with a smooth function. Horizontal lines show the 5σ and 95% CL levels.

- [3] **Phys. Rev. Lett.** **50**, 811 (1983), E. Eichten, K. Lane, and M. E. Peskin, “New Tests for Quark and Lepton Substructure”.
- [4] **Rev. Mod. Phys.** **56**, 579 (1984), **58**, 1065 (1986), E. Eichten, I. Hinchliffe, K. Lane, and C. Quigg, “Super-collider Physics”.
- [5] **hep-ph/9605257**, K. Lane, “Electroweak and Flavor Dynamics at Hadron Colliders”.
- [6] **CMS Note - 2006/071**, Selda Esen and Robert M. Harris, “CMS Sensitivity to Quark Contact Interactions using Dijets”.
- [7] **Phys. Commun.** **82**, 74 (1994), T. Sjöstrand “PYTHIA”.
- [8] **CMS-Note - 2006/067**, D. Acosta et al., “The Underlying Event at LHC”.
- [9] **CMS IN -2007/053**, M. Vázquez Acosta et al., “Jet and MET Performance in CMSSW_1_2_0”.
- [10] **CMS-Note - 2006/020**, R. Demina et al., “Calorimeter Cell Energy Thresholds for Jet Reconstruction in CMS”.

- [11] **Phys. Rev. Lett.** **82**, 2457 (1999), B. Abbott et al., “*Dijet Mass Spectrum and a Search for Quark Compositeness in $\bar{p}p$ Collisions at $\sqrt{s} = 1.8$ TeV*”.
- [12] **CMS Note - 2006/069**, Selda Esen, Robert M. Harris, “*Jet Triggers and Dijet Mass*”.
- [13] B. Bollen, M. Cardaci, R. Harris, “*Dijet resonance Studies and Dijet Selection Optimization*”, CMS analysis note in preparation.